J Electroceram (2011) 27:114–119
DOI 10.1007/s10832-011-9654-7

First-principle studies of the electronic structure and reflectivity of $LaTiO_3$ and Sr doped $LaTiO_3$ ($La_{1-x}Sr_xTiO_3$)

Li Hong Gao · Zhuang Ma · Qun Bo Fan

Received: 14 February 2011 / Accepted: 29 August 2011 / Published online: 16 September 2011

Abstract The electronic structures and optical properties of pure and Sr doped $LaTiO_3$ were studied using the first-principle density functional theory (DFT). The results show that the Fermi surface of $LaTiO_3$ lies in its conduction band, which makes its reflectivity (about 68.3% at the laser wavelength of 10.6 μm) much higher than other ceramic materials. Sr doping lowers the conduction band and reduces the band gap of $La_{1-x}Sr_xTiO_3$ which is beneficial to the prompt of reflectivity. We also found that shifting of the conduction band is not linear with Sr dopant concentration, and a minimum energy level is reached when x=0.25. For the reflectivity of $La_{1-x}Sr_xTiO_3$, it first increases and then decreases with increasing Sr concentration; a maximum reflectivity (99.2%) is achieved when x=0.25.

Keywords $La_{1-x}Sr_xTiO_3$ · First-principle · Energy band structure · Reflectivity

1 Introduction

Materials for laser equipment and protection components are desired to have high reflectivity and chemical stability at high temperatures. Ceramics are superior in terms of chemical stability, yet, in most cases, have lower reflectivity than metals. Therefore, it is necessary to develop ceramic materials with improved reflectivity.

As an important dielectric material for microwave and high frequency capacitor at high temperature [1], $LaTiO_3$ has attracted enormous attention for decades. It has a perovskite structure, and has good dielectric property which favors the reflectivity [2]. The existence of titanium $3d^1$ electron makes $LaTiO_3$ an essential Mott insulator [3] which has the metal insulator transformation (MIT). B.Vilquin et al. [4] has revealed that metal insulator transformation can occur in $LaTiO_3$ under the conditions of high temperature, oxide defects or certain types of dopant, such as Sr found by K. Yoshii et al. [5]. Furthermore, Tokura et al. [6, 7] and W. B Wu [8] have successful experiments to suggest that properly doped $La_{1-x}Sr_xTiO_3$ shows metallic conductivity at room temperature.

Up to now, studies of the $LaTiO_3$ based systems [9–11] are mainly focusing on the aspects of crystal structure, phase, electrical [12], magnetic, and ferroelectric properties. Less work has been done on the optical properties. To the best of our knowledge, no work on the investigation of optical properties of $LaTiO_3$ and $La_{1-x}Sr_xTiO_3$ with the aid of theoretical simulations has heretofore been reported.

In this paper, the electronic structures (energy band structure and density of states) and optical properties (reflectivity) of $LaTiO_3$ and $La_{1-x}Sr_xTiO_3$ have been studied using first-principle density functional theory (DFT) with the aid of the Cambridge Sequential Total Energy Package code (CASTEP) module of the Material Studio software. The effect of Sr dopant concentration on the reflectivity of $La_{1-x}Sr_xTiO_3$ is also studied. In this work, a wavelength of 10.6 μm [13] is selected, which is widely used in the laser industry.

L. H. Gao · Z. Ma (✉) · Q. B. Fan
School of Material Science and Engineering,
Beijing Institute of Technology,
Beijing 100081, China
e-mail: hstrong929@hotmail.com

L. H. Gao
Institut Fresnel,
UMR 6133 – CNRS Faculté des Sciences et Techniques,
Avenue Escadrille Normandie Niemen,
13397 Marseille Cedex 20, France

2 Computational methods and structure models

The reflectivity $R(\omega)$ of a material can be obtained from the complex dielectric function [14]. It follows the Fermi distribution [15] with the assumption that the crystal surface direction is parallel with the light axe, and is expressed as

$$\mathrm{R}(\omega) = \left| \frac{\sqrt{\varepsilon(\omega)} - 1}{\sqrt{\varepsilon(\omega)} + 1} \right|^2, \tag{1}$$

in which ω is frequency and $\varepsilon(\omega)$ is the complex dielectric function. The imaginary part $\varepsilon_2(\omega)$ of the complex dielectric function mainly contributes to the electronic structure which has a close relationship with the response of electrons, i.e., the interband transitions [16]. By calculating the overall transitions of electrons at k point from valence band to conduction band in the Brillouin zone, ε_2 is given by [16–18]:

$$\varepsilon_2(q \to 0, h\omega) = \frac{2e^2\pi}{\Omega\varepsilon_0} \sum \left| \langle \psi_k^c | \hat{u}, r | \psi_k^v \rangle \right|^2 \delta(E_K^C - E_K^V - E), \tag{2}$$

where Ω is the unit-cell volume, $\psi_k^c|\hat{u}, r|\psi_k^v$ is the location matrix, E_K^C and E_K^V are the electronic transition energies of the conduction band and the valence band, respectively, and E is the energy of a photon.

The real part $\varepsilon_1(\omega)$ of the complex dielectric function can be derived from $\varepsilon_2(\omega)$ by the Kramers-Kronig dispersion relationship [19], obtained from the principle of causality. The relationship between $\varepsilon_1(\omega)$ and $\varepsilon_2(\omega)$ is expressed as follows:

$$\varepsilon_1(\omega) = \varepsilon_{1\infty} + \frac{2}{\pi} P \int_0^\infty \frac{\omega' \varepsilon_2(\omega')}{\omega'^2 - \omega^2} \cdot d\omega', \tag{3}$$

where $\varepsilon_{1\infty}$ is ε_1 at high frequency, and P denotes Cauchy's principal value integral. Based upon Eqs. 1, 2 and 3, the reflectivity of materials can be derived.

The calculations are carried out by the ultrasoft pseudopotential plane-wave method of the CASTEP module based on the first-principle density function theory (DFT). The exchange–correlation contribution is described by the generalized gradient approximation (GGA) proposed by Perdew et al. [20]. It's used to calculate the Kohn-Sham equations for obtaining the ground state density and the total energy of the multiple electrons system. An energy cutoff of 300 eV and an energy accuracy of 2.0×10^{-6} eV/atom were used for our calculations. Only the valence electrons are taken into account, corresponding to La $5s^2$ $5p^6$ $5d^1$ $6s^2$, Sr $4s^2$ $4p^6 5s^2$, Ti $3s^2 3p^6 3d^2 4s^2$ and O $2s^2 2p^4$.

Crystal structures are also required for the calculation. $LaTiO_3$ has a cubic perovskite crystal structure (Fig. 1). It belongs to *PM*-3*M* space group with lattice parameter 3.92 Å [21]. The La ions are located at the eight corners of the cubic unit cell, and the O ions are located at the centers of the six facets. The smallest Ti ion resides in the center of the oxygen octahedron.

The $La_{1-x}Sr_xTiO_3$ model is constructed by partially replacing La ions with Sr ions. In order to analyze the effect of variable Sr concentration, super-lattices, with some of the La ions replaced by Sr ions, are constructed. These super-lattices are created by multiplying the unit cells along the *x*, *y* and *z* axes. Considered the computational efficiency and reliability of results, the models of $La_{0.875}Sr_{0.125}TiO_3$, $La_{0.75}Sr_{0.25}TiO_3$, $La_{0.5}Sr_{0.5}TiO_3$ and $La_{0.25}Sr_{0.75}TiO_3$ are built as displayed in Fig. 2. The fact that cation ordering, i.e. La and Sr are ordered with respect to each other, does not have any effect on the material's reflectivity has been proved, so one structure for each Sr dopant concentration is demonstrated in this paper.

3 Results and discussion

3.1 Electronic structure and reflectivity of $LaTiO_3$

Figure 3 presents the energy band structure and density of states (DOS) of $LaTiO_3$, the symmetric points of which are *X*, *R*, *M* and *G*, respectively. The fact that the top of the valence band and the bottom of the conduction band coincide at point *G* suggests $LaTiO_3$ is a direct bandgap semiconductor material. The band gap between valence band and conduction band is 1.3 eV.

As shown in Fig. 3, the Fermi level of $LaTiO_3$, the energy of which is set to 0 eV, lies in the conduction band. This can be explained by our previous work [22]. In the series of titanate ($ATiO_3$), such as $CaTiO_3$, $SrTiO_3$ and $BaTiO_3$, the conduction band moves to a lower energy level with increasing atomic number of the cation located at the A site, and the Fermi level moves to a higher energy level simultaneously. If the atomic number of *A* is great enough,

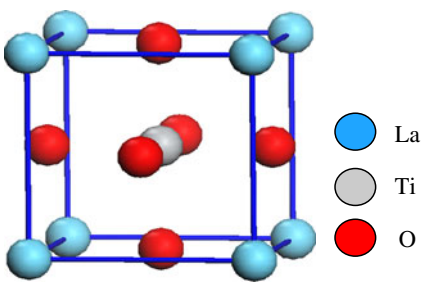

Fig. 1 Crystal structure of $LaTiO_3$

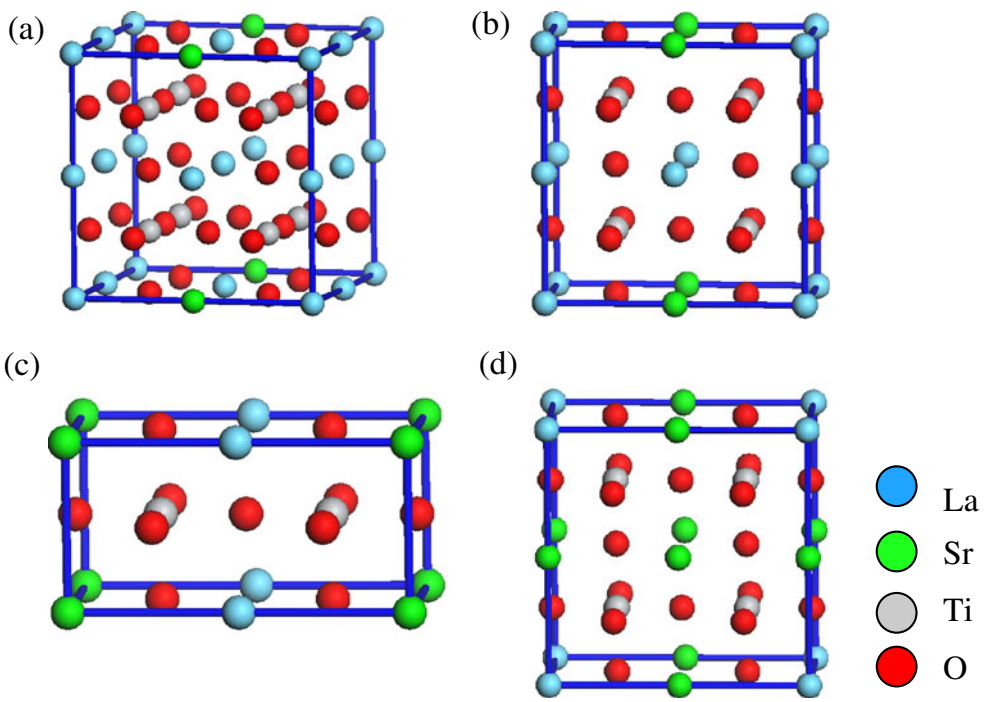

Fig. 2 Crystal structure of $La_{1-x}Sr_xTiO_3$ (**a**) $La_{0.875}Sr_{0.125}TiO_3$ (**b**) $La_{0.75}Sr_{0.25}TiO_3$ (**c**) $La_{0.5}Sr_{0.5}TiO_3$ (**d**) $La_{0.25}Sr_{0.75}TiO_3$

for example La, the Fermi level can move into the conduction band.

The entrance of Fermi level into conduction band can be further demonstrated by the partial density of states (PDOS) as displayed in Fig. 4. The Fermi level of the PDOS of La enters into the 5*d* and the 3*d* states of Ti and 2*p* state of O. The total DOS of $LaTiO_3$ is obtained by the sum of these three PDOS, which shows that the Fermi level locates in the conduction band.

The construction of energy band structure can be seen from the comparison of total DOS and PDOS. Due to the importance of the valence band and conduction band, Fig. 4 just focuses on the energy bands near the Fermi level. In fact, in the total DOS four energy bands exist below Fermi energy level. One ranging from −59.0 eV to −57.1 eV is attributed to Ti 3*s* state. And La 5*s* and Ti 3*p* states dominate the one in the range of −36.1 eV~−33.7 eV. One from −22.2 eV to −16.8 eV is mainly attributed to La 5*p* and O 2*s* states. The valence band in the range of −9.1 eV~−3.0 eV is essentially formed by O 2*p* state. Finally, the conduction band spreads a large energy range of −1.7 eV~14.0 eV. It can be noted in Fig. 4 that the conduction band displays an obvious hybridization of La 5*p* 5*d* 6*s*, Ti 3*d* and O 2*p*.

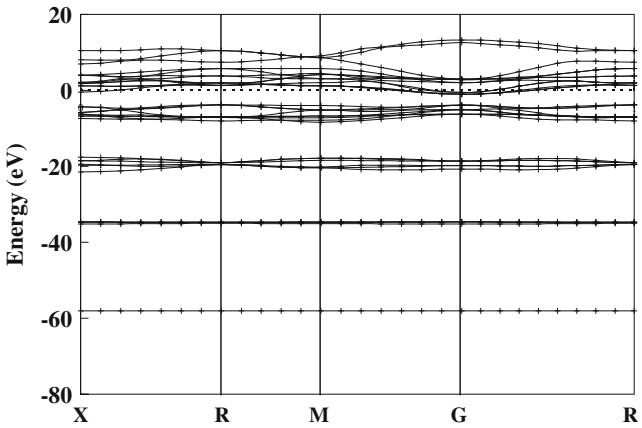

Fig. 3 Energy band structure of $LaTiO_3$

The reflectivity of $LaTiO_3$ has been investigated. At the wavelength of 10.6 μm the reflectivity is 68.3%. This value is fairly high for a ceramic material. It can be explained that both the imaginary part and real part of the dielectric function influence the reflectivity. A high real and imaginary parts of the dielectric function tend to improve the reflectivity according to our previous work [23], as can be concluded from Eq. 1. Due to the excellent dielectric function of $LaTiO_3$, its reflectivity is higher than most other ceramic materials. Furthermore, the radical reason can be found from the energy band structure. Because of the entrance of Fermi level into the conduction band, most excited electrons rotate closely to the conduction band, and some of them are situated in the conduction band. Consequently, the interband transitions can more easily occur in these excited electrons. This phenomenon is responsible for the good, metallic-like reflective properties observed in this material.

Besides *PM*-3*M* space group, the reflectivity of $LaTiO_3$ with *PBNM* space group was also calculated. The calculated reflectivity at the wavelength of 10.6 μm, 30.8%, agrees very well with the experimental value, 30%–35% [24]. So the reflectivity calculation is reliable.

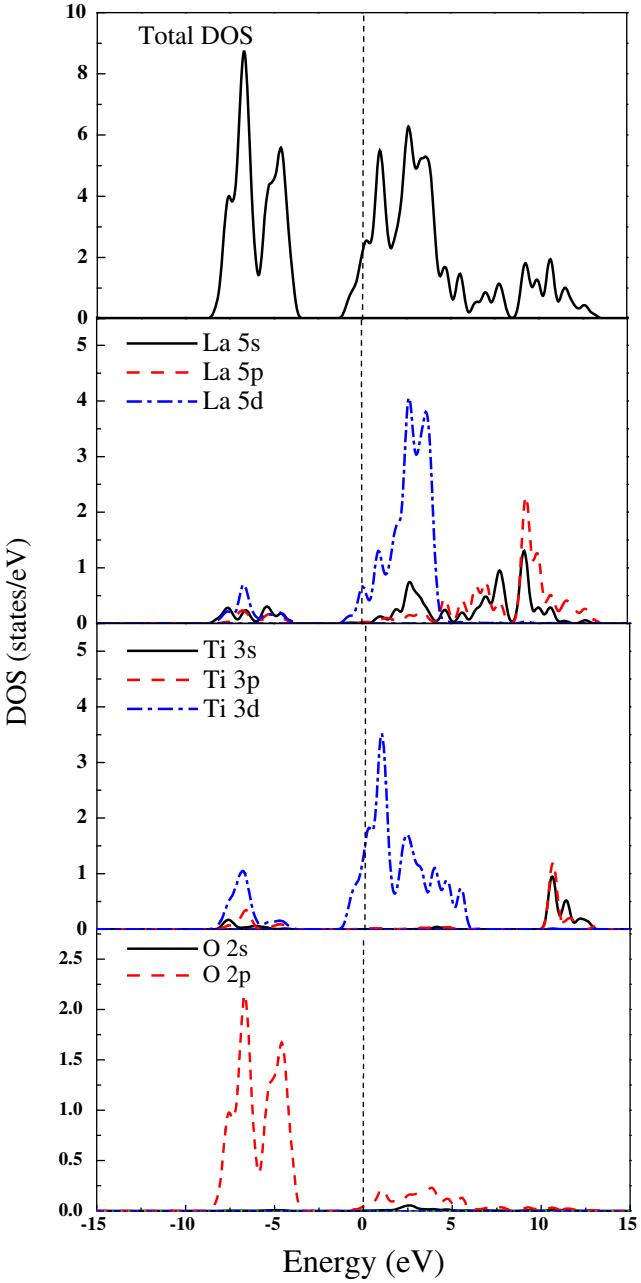

Fig. 4 Total and partial DOS of $LaTiO_3$

3.2 Electronic structure and reflectivity of Sr doped $LaTiO_3$

3.2.1 Electronic structures of $La_{1-x}Sr_xTiO_3$ with varying Sr concentrations

From the DOS calculation, we see that $La_{1-x}Sr_xTiO_3$ has the same numbers of energy bands as $LaTiO_3$: four energy bands below the Fermi level and one conduction band above. The total DOS of $La_{1-x}Sr_xTiO_3$ with varying Sr concentrations is shown in Fig. 5.

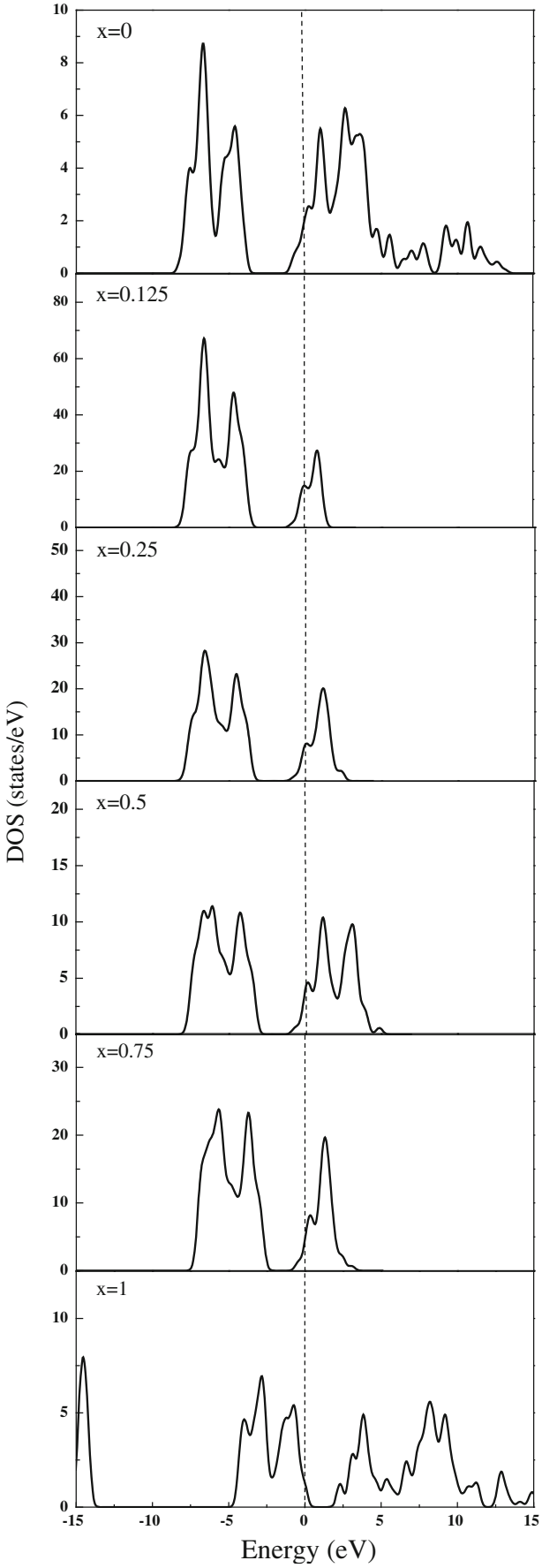

Fig. 5 Total DOS of $La_{1-x}Sr_xTiO_3$

We focus on the Fermi level, conduction band and its band gap, because they play a key role in the energy band structure and optical property. We notice that the Fermi level of $La_{1-x}Sr_xTiO_3$ is still in the conduction band, yet its energy distribution is different from $LaTiO_3$ (this can be inferred by the energy at which the bottom of the conduction band lies, as shown in Table 1). The energy at the conduction band bottom first decreases with increasing Sr dopant concentration. That means the conduction band moves to a lower energy level and the corresponding Fermi level moves to a higher energy level. When x reaches 0.25, the energy at the bottom of the conduction band goes through a minimum. Further increase of Sr dopant (x increased from 0.5 to 1) will move up the energy level of the conduction band bottom, indicating the conduction band moves to the opposite direction (the higher energy) and the Fermi level moves to the lower energy direction. When x equals to 1, (i.e., $SrTiO_3$) the conduction band is above the Fermi level.

The band gap of $La_{1-x}Sr_xTiO_3$ as a function of Sr dopant concentration is shown in Fig. 6. The band gap reduces with increasing Sr concentration, a phenomenon attributed to the difference of electronic configuration between Sr and La. Lacking of one electron, Sr can provide a bare energy orbit that can form an acceptor energy band located in between the conduction band and valence band, and hence reduces the band gap.

3.2.2 Reflectivity of $La_{1-x}Sr_xTiO_3$ with varying Sr concentrations

The reflectivity of $La_{1-x}Sr_xTiO_3$ as a function of Sr dopant concentration is shown in Fig. 7. It can be observed that the reflectivity first increases with increasing Sr concentration till reaches a maximum of 99.2% when x=0.25. This is an extremely high reflectivity value which is comparable to the reflectivity of metals such as gold or aluminum. The reflectivity begins to decrease when x exceeds 0.25, and falls to merely 8.5% when x equal to 0.75.

Such a change in reflectivity vs. Sr concentration is attributed to two aspects. On the one hand, as we already mentioned, the conduction band moves to the lower energy level when x is smaller than 0.25, and the number of active valence electrons below the Fermi level increases; consequently, the number of electrons that could participate in the interband transitions increases. As we all know that reflection occurs when the excited electrons in the higher energy band jump into the lower energy band; therefore, the more interband transitions, the more reflection processes occur. On the other hand, the band gap reduces when x is smaller than 0.25; this will make the interband transitions occur more easily. As a result, the reflectivity is enhanced. However, when x approaches to 0.5, 0.75 and 1, the conduction band moves to the opposite direction-the higher energy band, which leads to a decrease in the numbers of electrons that can participate in the interband transitions. Although the reduction in band gap energy is favorable to

Table 1 Energy at the bottom of conduction band of $La_{1-x}Sr_xTiO_3$

x	Energy at the bottom of conduction band (eV)
0	−1.73
0.125	−1.78
0.25	−1.79
0.5	−1.73
0.75	−1.47
1	0.99

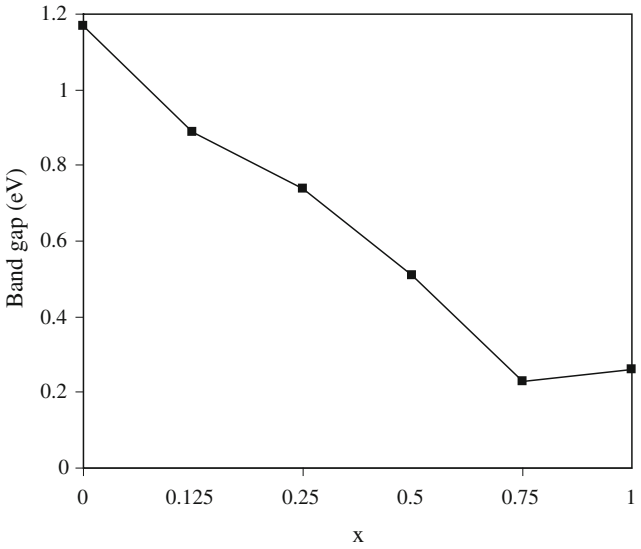

Fig. 6 Band gap of $La_{1-x}Sr_xTiO_3$ as a function of Sr doping concentration

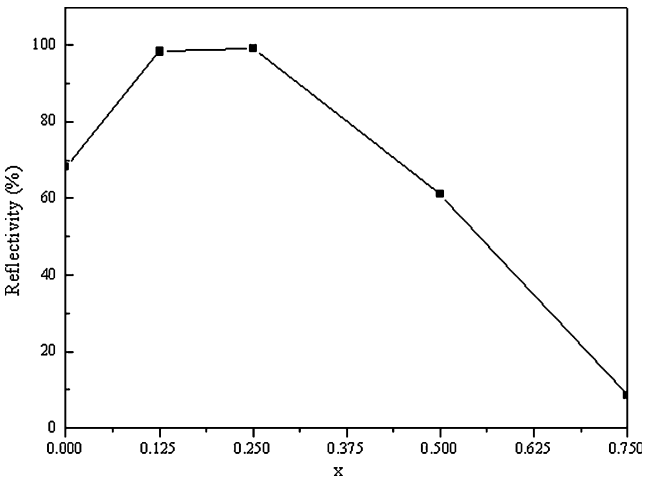

Fig. 7 Reflectivity of $La_{1-x}Sr_xTiO_3$ at the wavelength of 10.6 μm as a function of Sr doping concentration

the interband transitions of electrons, competition of these two effects decreases the reflectivity of the material [25].

4 Conclusions

This paper has investigated the electronic structures and reflectivity of pure and Sr doped $LaTiO_3$ by employing first-principle GGA-based Density Functional Theory calculations, with ultrasoft pseudopotentials. Results show that $LaTiO_3$ belongs to the direct band gap semiconductor material with a band gap energy about 1.3 eV. A high dielectric function is favorable to achieve high reflectivity, and a reflectivity of 68.3% has been observed at the wavelength of 10.6 μm. The entrance of Fermi level into the conduction band introduces active electrons close to and some inside the conduction band. The interband transition of these electrons is the reason for its as-metal behavior in terms of reflectivity.

Introduction of Sr in $LaTiO_3$ ($La_{1-x}Sr_xTiO_3$) lowers the conduction band, and a minimum energy is achieved when x=0.25. Sr doping also reduces the band gap by forming an acceptor energy band. An ultrahigh reflectivity of 99.2% is observed in $La_{0.75}Sr_{0.25}TiO_3$, an effect attributed to the lowering of conduction band and reduction in the band gap.

Acknowledgements This work is supported by Beijing Institute of Technology funded grant B00347.

References

1. A.N. Salak, M.P. Seabra, V.M. Ferreira, J. Eur. Ceram. Soc. **23**, 2409 (2003)
2. Y.F. Qu, *Functional Ceramics and Application* (Chemical Industry Press, Beijing, 2003)
3. N.F. Mott, *The Metal–Insulator Transition* (Taylor and Francis, London, 1974)
4. B. Vilquin, T. Kanki, T. Yanagida, H. Tanaka, T. Kawai, Solid State Commun. **136**, 328 (2005)
5. A. Nakamura, K. Yoshii, H. Abe, J. Alloys Compd. **290**, 236 (1999)
6. Y. Tokura, Y. Taguchi, Y. Okada, Y. Fujishima, T. Arima, K. Kumagai, Y. Iye, Phys. Rev. Lett. **70**, 2126 (1993)
7. K. Kumagai, T. Suzuki, Y. Taguchi, Y. Okada, Y. Fujishima, Y. Tokura, Phys. Rev. B **48**, 7636 (1993)
8. W.B. Wu, F. Lu, J. Appl. Phys. **88**, 700 (2000)
9. W.Z. Yang, M.M. Mao, X.Q. Liu, X.M. Chen, J. Appl. Phys. **107**, 124102 (2010)
10. V.R. Mastelaro, Y.P. Mascarenhas, P.P. Neves, M. Mir, A.C. Doriguetto, A. Michalowicz, J. Moscovici, M.H. Lente, J.A. Eiras, J. Appl. Phys. **107**, 114103 (2010)
11. X.H. Hao, J.W. Zhai, F. Shang, J. Zhou, S.L. An, J. Appl. Phys. **107**, 116101 (2010)
12. S. Ohta, T. Nomura, H. Ohta, K. Koumoto, J. Appl. Phys. **97**, 034106 (2005)
13. C.K.N. Patel, Phys. Rev. **136**, A1187 (1964)
14. P.S. Xu, C.K. Xie, H.B. Pan, F.Q. Xu, J. Electron. Spectrosc. Relat. Phenom. **144–147**, 593 (2005)
15. L.P. Peng, L. Xu, J.W. Yin, Acta Phys. Sin. **56**, 1585 (2007)
16. Y.L. Li, W.L. Fan, H.G. Sun, X.F. Cheng, P. Li, X. Zhao, J. Appl. Phys. **107**, 093506 (2010)
17. S. Saha, T.P. Sinha, Phys. Rev. B **62**, 8828 (2000)
18. C.H. Tang, M.Q. Cai, Y.K. Cui, J NanJing Normal University (Natural Science) **29**, 40 (2006)
19. J. Petalas, S. Logothetidis, M. Gioti, C. Janowitz, Phys. Stat. Sol. B **209**, 499 (1998)
20. J.P. Perdew, K. Burke, M. Ernzerhof, Phys. Rev. Lett. **77**, 3865 (1996)
21. M. Kestigian, R. Ward, J. Am. Chem. Soc. **76**, 6027 (1954)
22. L. H. Gao, The research of the laser reflectivity of functional ceramics, Master thesis, in *School of Material Science and Engineering*, (Beijing Institute of Technology, Beijing, 2009).
23. L.H. Gao, F.C. Wang, Z. Ma, Y.B. Liu, D.R. Li, L.N. Shen, Rare Met. Mat. Eng. **38**, 773 (2009)
24. D.A. Crandles, T. Timusk, J.E. Greedan, Phys. Rev. B **44**, 13250 (1991)
25. X.D. Zhang, M.L. Guo, W.X. Li, C.L. Liu, J. Appl. Phys. **103**, 063721 (2008)